SUPPLEMENTARY INFORMATION

The *S. pombe* mRNA decapping complex recruits cofactors and a previously unidentified activator through a single dynamic surface.

Jan Philip Wurm, Jan Overbeck, Remco Sprangers*

Max Planck Institute for Developmental Biology, Spemannstrasse 35, 72076 Tübingen, Germany

Figure S1

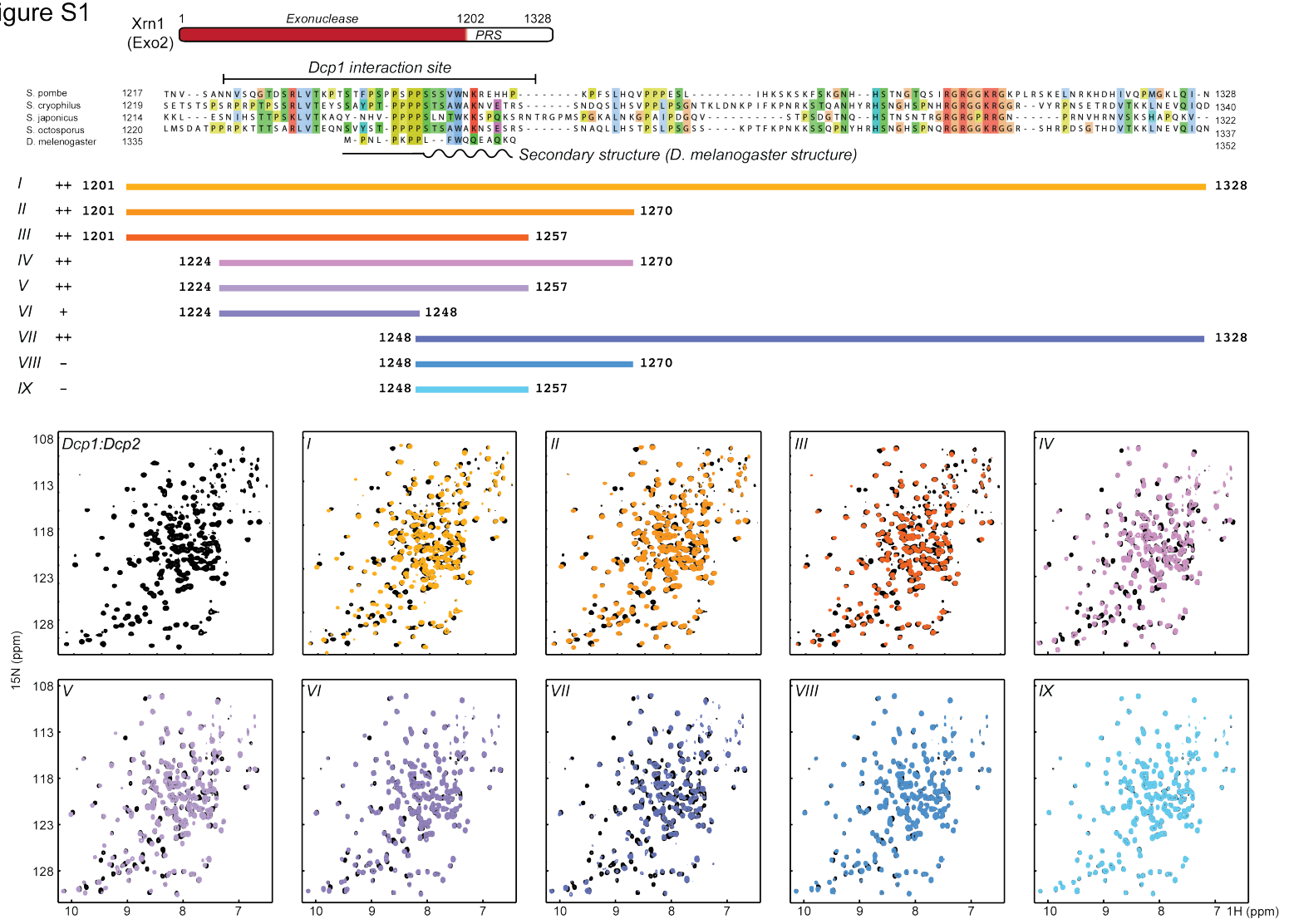
Xrn1
(Exo2)
1
Exonuclease
1202
1328
PRS
Dcp1 interaction site
S. pombe 1217 1328
S. cryophilus 1219 1340
S. japonicus 1214 1322
S. octosporus 1220 1337
D. melenogaster 1335 1352
Secondary structure (D. melanogaster structure)
I ++ 1201 1328
II ++ 1201 1270
III ++ 1201 1257
IV ++ 1224 1270
V ++ 1224 1257
VI + 1224 1248
VII ++ 1248 1328
VIII – 1248 1270
IX – 1248 1257
Dcp1:Dcp2
I
II
III
IV
V
VI
VII
VIII
IX
15N (ppm)
1H (ppm)

FIGURE S1: Interactions between Xrn1 and the Dcp1:Dcp2 decapping complex. (top) Cartoon of the protein and sequence alignment of the C-terminal region of Xrn1 from several *Schizosaccharomyces* species. The *D. melanogaster* sequence from which structural information in complex with Dcp1 is known, is indicated. (middle) Constructs used for NMR titration experiments. The strength of the interaction is indicated (++ : strong binding, +: binding, - : no binding). (bottom) NMR spectra where a three fold excess of unlabeled Xrn1 is added to the ^{15}N labeled decapping complex.

Figure S2

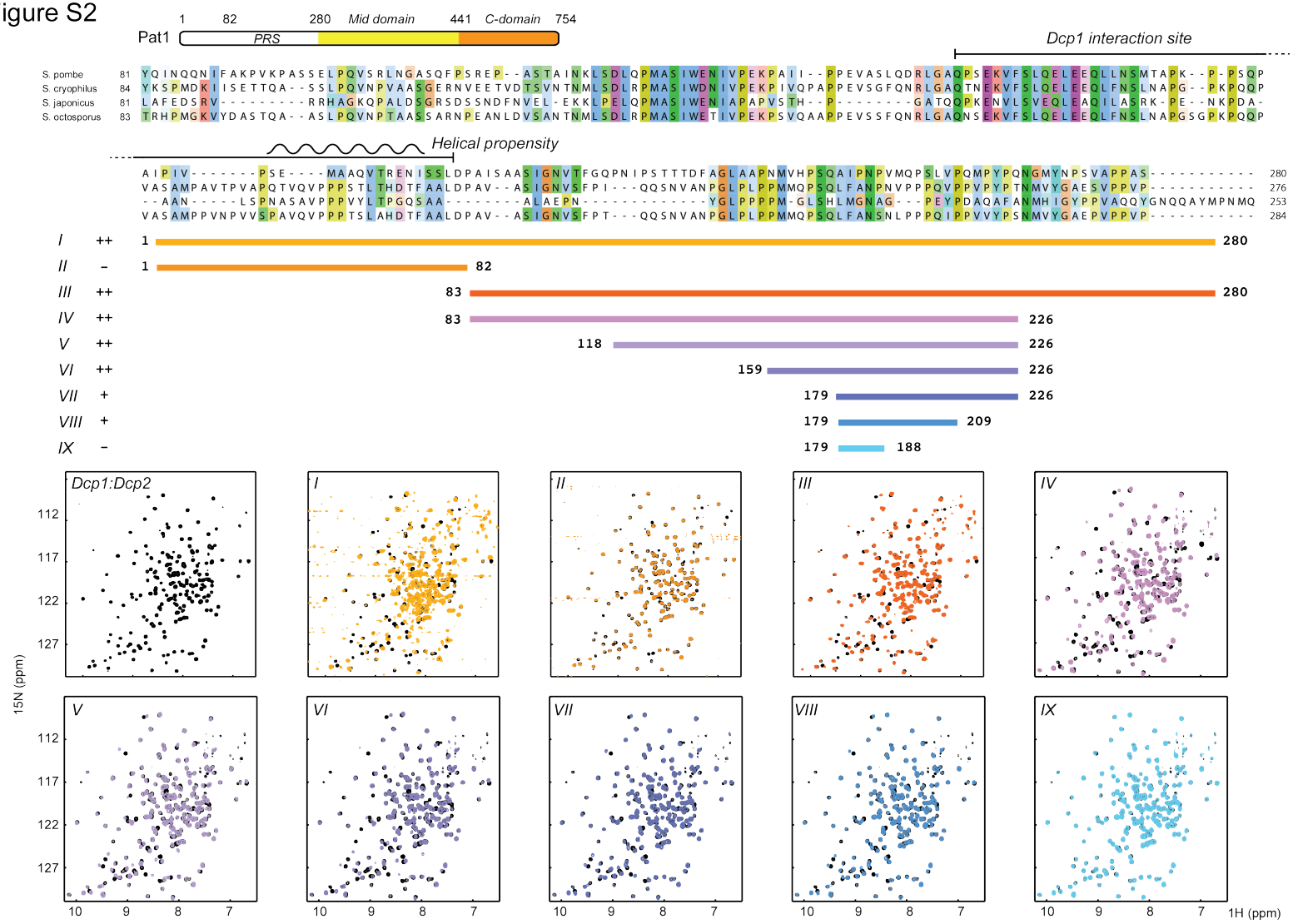
Pat1
1
82
280
Mid domain
441
C-domain
754
PRS
Dcp1 interaction site
S. pombe
S. cryophilus
S. japonicus
S. octosporus
Helical propensity
I ++ 1 280
II – 1 82
III ++ 83 280
IV ++ 83 226
V ++ 118 226
VI ++ 159 226
VII + 179 226
VIII + 179 209
IX – 179 188
Dcp1:Dcp2
I
II
III
IV
V
VI
VII
VIII
IX
15N (ppm)
1H (ppm)

FIGURE S2: Interactions between Pat1 and the Dcp1:Dcp2 decapping complex. (top) Cartoon of the protein and sequence alignment of the N-terminal region of Pat1 from several *Schizosaccharomyces* species. (middle) Constructs used for NMR titration experiments. The strength of the interaction is indicated (++ : strong binding, +: binding, - : no binding). (bottom) NMR spectra where a three fold excess of unlabeled Pat1 is added to the ^{15}N labeled decapping complex.

Figure S3

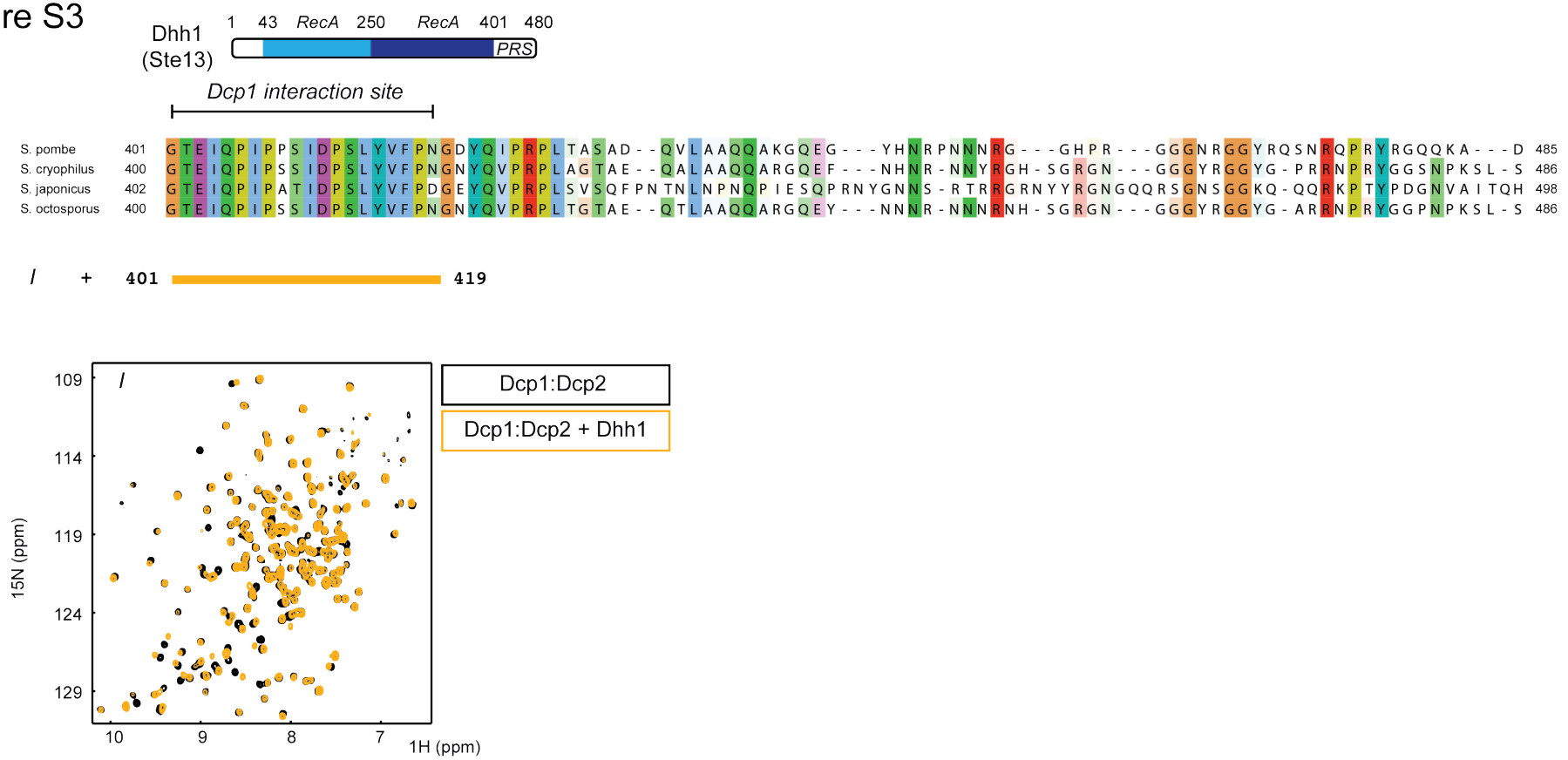
Dhh1
(Ste13)
1
43
RecA
250
RecA
401
480
PRS
Dcp1 interaction site
S. pombe 401 GTEIQPIPPSIDPSLYVFPNGDYQIPRPLTASAD--QVLAAQQAKGQEG---YHNRPNNNRG---GHPR---GGGNRGGYRQSNRQPRYRGQQKA---D 485
S. cryophilus 400 GTEIQPIPSSIDPSLYVFPNGNYQVPRPLAGTAE--QALAAQQARGQEF---NHNR-NNYRGH-SGRGN---GGGYRGGYG-PRRNPRYGGSNPKSL-S 486
S. japonicus 402 GTEIQPIPATIDPSLYVFPDGEYQVPRPLSVSQFPNTNLNPNQPIESQPRNYGNNS-RTRRGRNYYRGNGQQRSGNSGGKQ-QQRKPTYPDGNVAITQH 498
S. octosporus 400 GTEIQPIPSSIDPSLYVFPNGNYQVPRPLTGTAE--QTLAAQQARGQEY---NNNR-NNNRNH-SGRGN---GGGYRGGYG-ARRNPRYGGPNPKSL-S 486
I + 401 419
I
109
114
119
124
129
15N (ppm)
10
9
8
7
1H (ppm)
Dcp1:Dcp2
Dcp1:Dcp2 + Dhh1

FIGURE S3: Interactions between Dhh1 and the Dcp1:Dcp2 decapping complex. (top) Cartoon of the protein and sequence alignment of the C-terminal region of Dhh1 from several *Schizosaccharomyces* species. (middle) Construct used for the NMR titration experiment. The strength of the interaction is indicated (+: binding). (bottom) NMR spectra where a three fold excess of unlabeled Dhh1 is added to the ^{15}N labeled decapping complex.

Figure S4

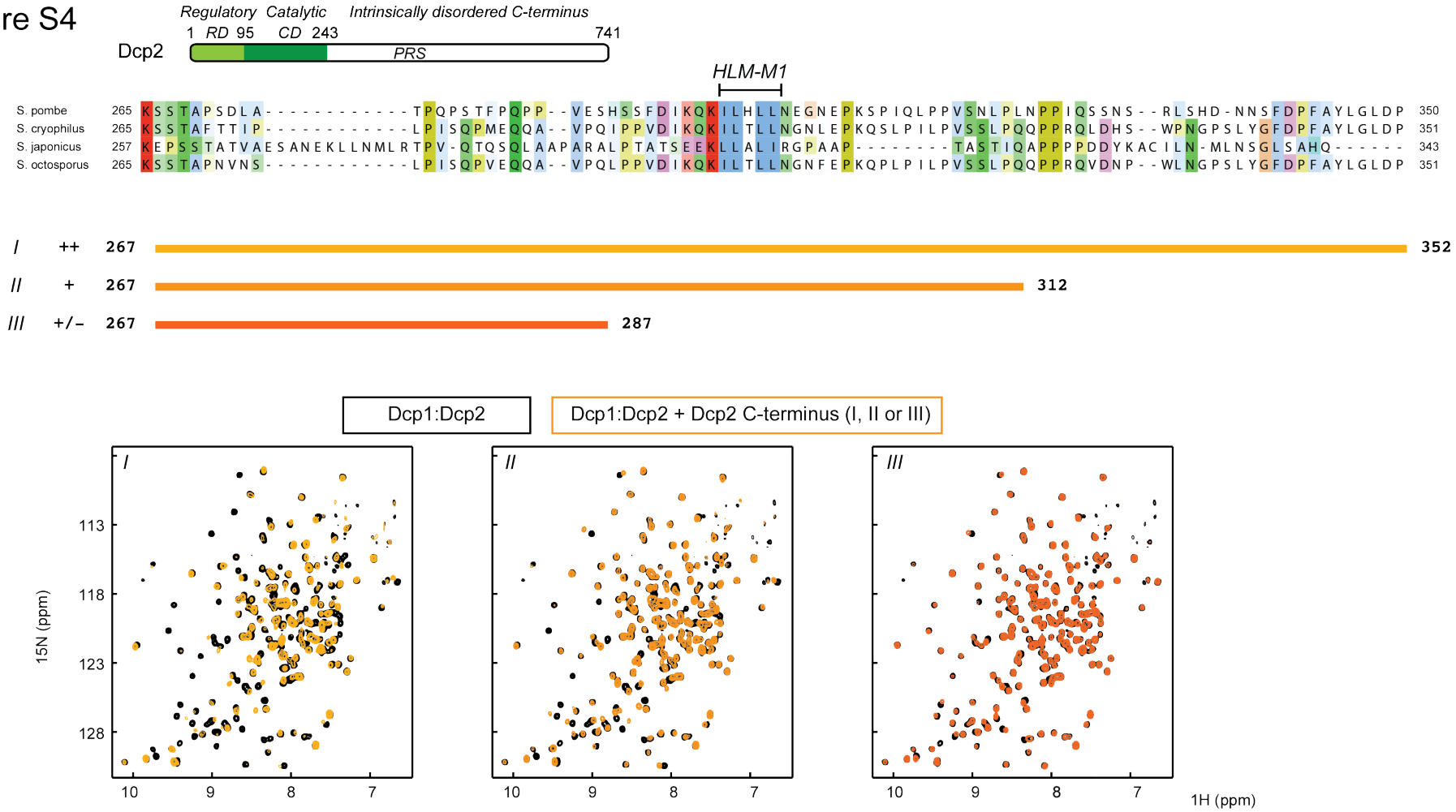
Regulatory
Catalytic
Intrinsically disordered C-terminus
1 RD 95
CD 243
741
Dcp2
PRS
HLM-M1
S. pombe 265 KSSTAPSDLA----------TPQPSTFPQPP--VESHSSFDIKQKILHLLNEGNEPKSPIQLPPVSNLPLNPPIQSSNS--RLSHD-NNSFDPFAYLGLDP 350
S. cryophilus 265 KSSTAFTTIP----------LPISQPMEQQA--VPQIPPVDIKQKILTLLNGNLEPKQSLPILPVSSLPQQPPRQLDHS--WPNGPSLYGFDPFAYLGLDP 351
S. japonicus 257 KEPSSTATVAESANEKLLNMLRTPV-QTQSQLAAPARALPTATSEEKLLALIRGPAAP--------TASTIQAPPPPDDYKACILN-MLNSGLSAHQ------ 343
S. octosporus 265 KSSTAPNVNS----------LPISQPVEQQA--VPQLPPVDIKQKILTLLNGNFEPKQPLPILPVSSLPQQPPRQVDNP--WLNGPSLYGFDPFAYLGLDP 351
I ++ 267 352
II + 267 312
III +/– 267 287
Dcp1:Dcp2
Dcp1:Dcp2 + Dcp2 C-terminus (I, II or III)
I
II
III
15N (ppm)
113
118
123
128
10
9
8
7
1H (ppm)

FIGURE S4: Interactions between the C-terminal region of Dcp2 and the Dcp1:Dcp2 decapping complex. (top) Cartoon of the protein and sequence alignment of the PRS in the C-terminal region of Dcp2 from several *Schizosaccharomyces* species. (middle) Constructs used for NMR titration experiments. The strength of the interaction is indicated (++ : strong binding, +: binding, +/- : weak binding). (bottom) NMR spectra where a three fold excess of unlabeled Dcp2 peptides is added to the ^{15}N labeled decapping complex. Note the disappearance of the Dcp1:Dcp2 signals in spectrum *I*, which is due to the peptide that is binding in different registers inside the Dcp1 aromatic groove.

Figure S5

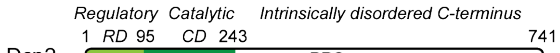

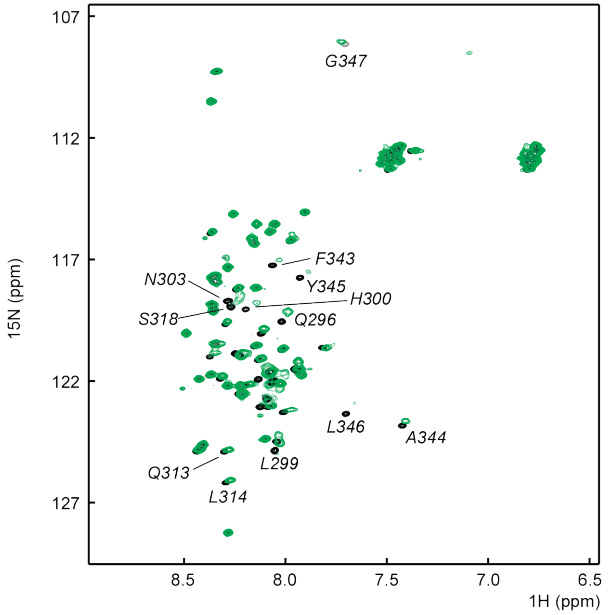

Dcp2 (*S. pombe*) residue 267-350

Dcp2 (*S. pombe*) residue 267-350 + Dcp1 (*S. pombe*)

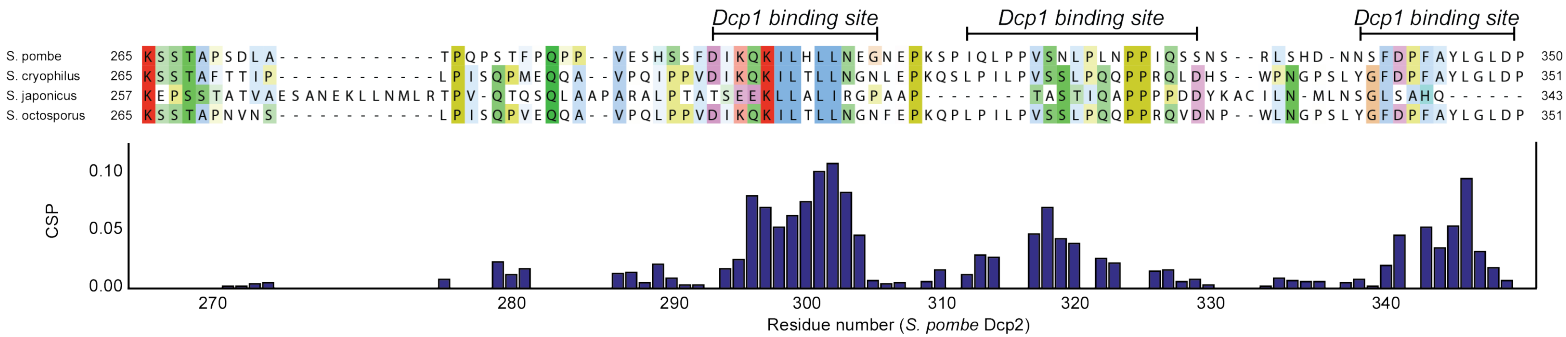

FIGURE S5: Interactions between the C-terminal region of Dcp2 and Dcp1. (top) Cartoon of the Dcp2 protein. (middle) NMR spectra of the Dcp2 C-terminal region in the absence (black) and presence (green) of a 1.4 fold excess of Dcp1. Some assignments are indicated. (bottom) CSP in the Dcp2 C-terminal region that are induced by Dcp1 plotted v/s the sequence of the protein. The sequence alignment of Dcp2 from several *Schizosaccharomyces* species is indicated as a reference.

Figure S6

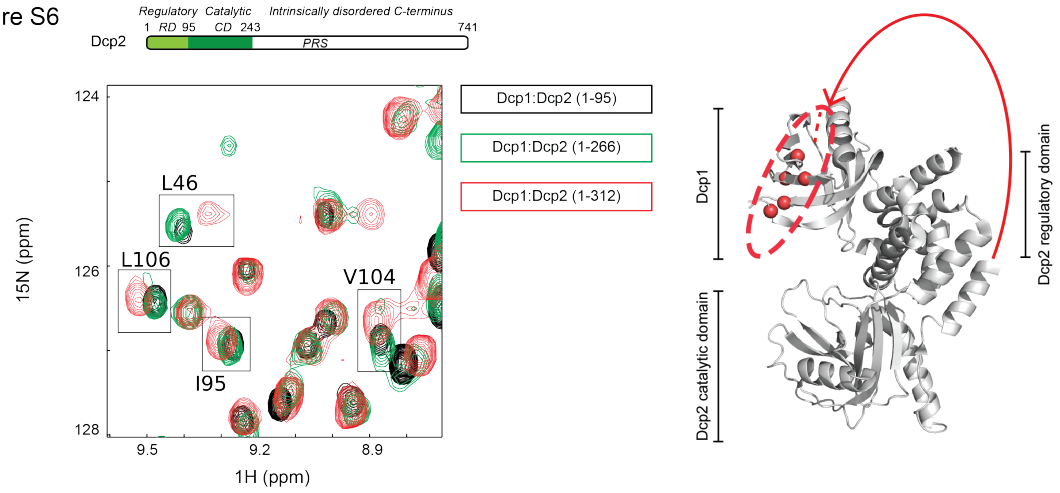

FIGURE S6: The interaction *in cis* between the C-terminal Dcp2 region and Dcp1. (left) NMR spectra of Dcp1:Dcp2 of increasing length. Dcp2 contains residues up to amino acid 95 (black, regulatory domain), 266 (green, regulatory + catalytic domains) and 312 (regulatory + catalytic domains + PRS). Upon inclusion of the PRS the residues in the Dcp1 aromatic groove experience CSPs. (right) Residues that experience CSP due to the PRS in Dcp2 are indicated with spheres on a cartoon of the Dcp1:Dcp2 structure. The predicted path of the Dcp2 PRS is indicated with a red line.

Figure S7

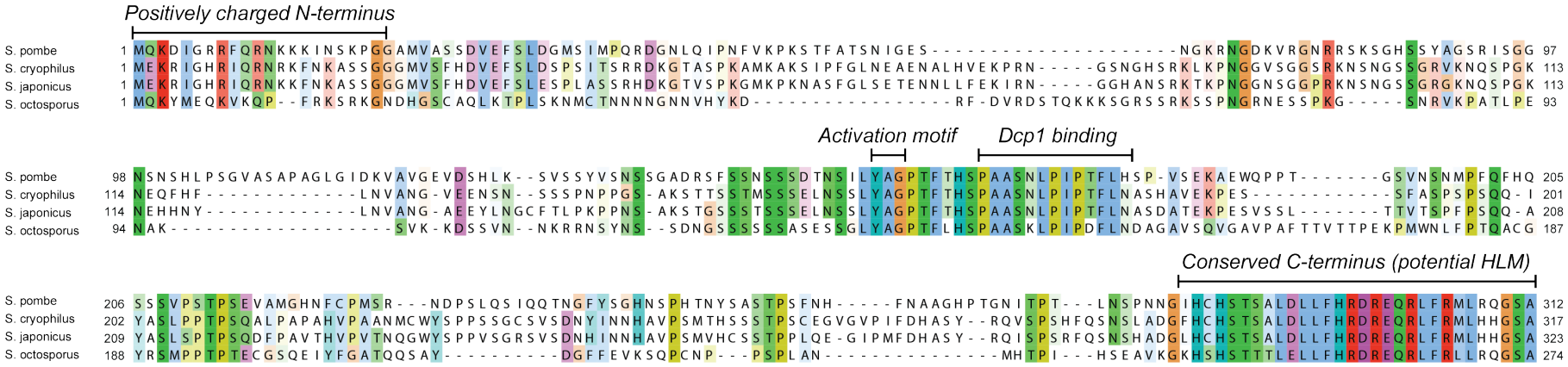
Positively charged N-terminus
Activation motif
Dcp1 binding
Conserved C-terminus (potential HLM)
S. pombe
S. cryophilus
S. japonicus
S. octosporus

FIGURE S7: Sequence alignment of Edc1 from several *Schizosaccharomyces* species. The positively charged N-terminal region, the activation motif, the Dcp1 interaction motif and the potential C-terminal HLMs are indicated.

Figure S8

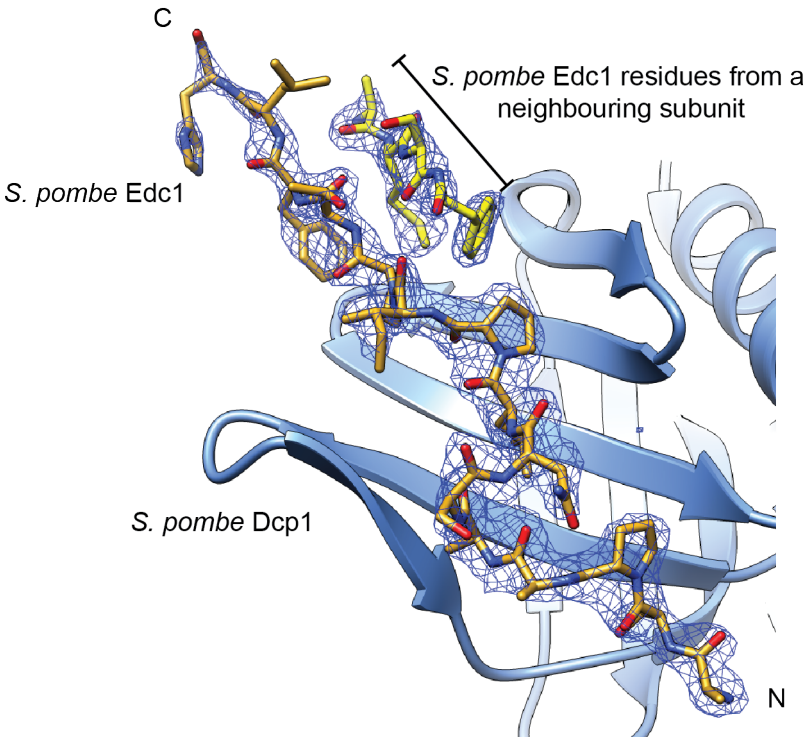

Figure S8. Crystal structure of the Dcp1:Edc1 complex. Dcp1 is displayed in blue. The Edc1 Dcp1 interaction motif is displayed in orange. A part of the N-terminal region of the Edc1 protein (that includes two amino acids from the cloning strategy) is visible (yellow). These residues arise from the Edc1 peptide in a symmetry related complex. These 4 amino acids are a crystallization artifact and likely of no biological relevance. The electron density ($2F_o$-F_c at 1.3 σ) is indicated with a blue mesh.

Figure S9

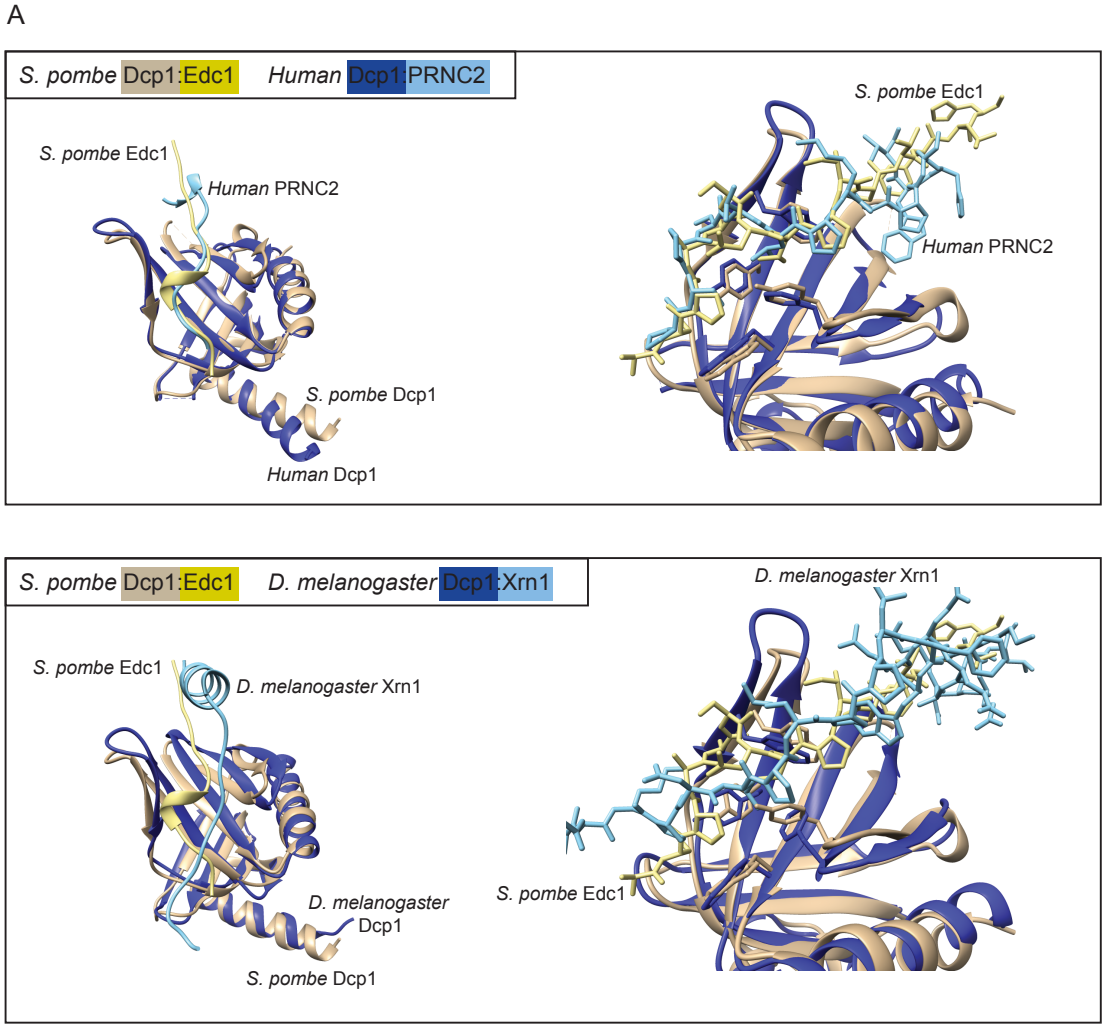

Figure S9: (A) Comparison of the Dcp1:Edc1 structure that we solved here (5JP4) with the structures of human Dcp1 in complex with PRNC2 (4B6H) (top) and of *D. melanogaster* Dcp1 in complex with Xrn1 (2LYD) (bottom). The Dcp1:Edc1 and Dcp1:PRNC2 structures overlap very well, even for the peptide. The Dcp1:Edc1 and Dcp1:Xrn1 complexes are different as Edc1 and

Xrn1 adopt significantly different conformation when bound to Dcp1. (B) Sequence alignment of the PRS motifs that we identified in the *S. pombe* proteins Xrn1, Pat1, Dhh1 and Dcp2 (2 motifs) (see Figure S1-S5). For comparison the sequence of *D. melanogaster* Xrn1 (see panel A) has been included. The *S. pombe* Edc1 protein is shown as a reference. The central PxPP motif is well conserved, whereas the region C-terminal to this motif is not aligned as it shows very limited conservation. In most cases, this region, however, has helical propensity in agreement with the structure of the *D.m.* Dcp1:Xrn1 structure (see above). To emphasize the structural differences between the Dcp1:Edc1 and the Dcp1:Xrn1 complexes the sequence C-terminal to the Edc1 PRS is not shown in the alignment.

Figure S10

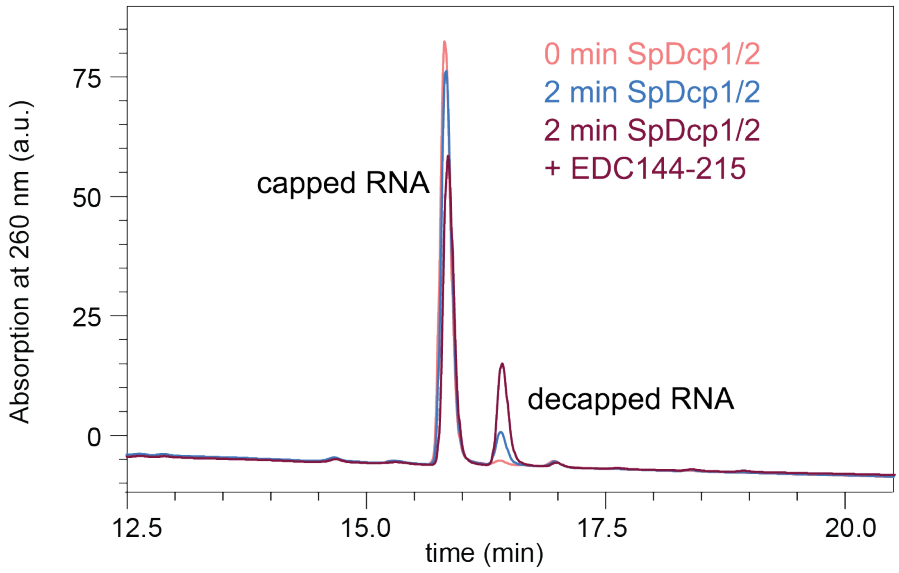

Figure S10. Exemplary HPLC traces of mRNA decapping reactions. The capped RNA (substrate) elutes around 15.8 min, whereas the decapped RNA (product) elutes at 16.5 minutes (see methods). The concentration of substrate and product depends on the enzyme complex used and on the reaction time.

Figure S11

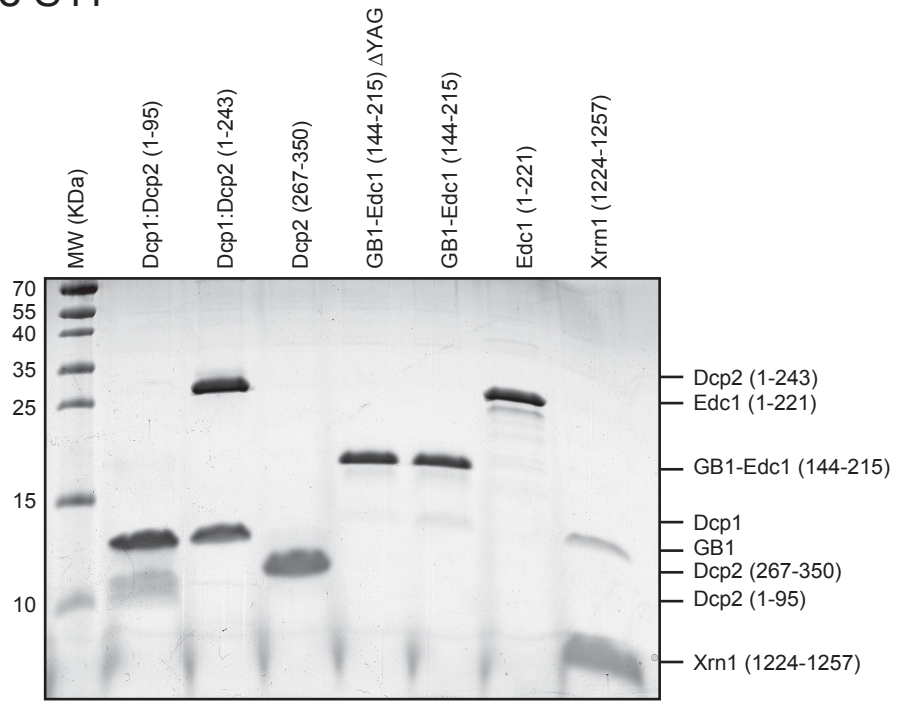

Figure S11. SDS PAGE analysis of the purified proteins used in the binding and activity assays that are presented in this manuscript. Xrn1 is contaminated with a small amount of the 6-His-GB1-purification tag. This tag does not interact with Dcp1 or Dcp2 and does thus not interfere with the experiments.

Figure S12

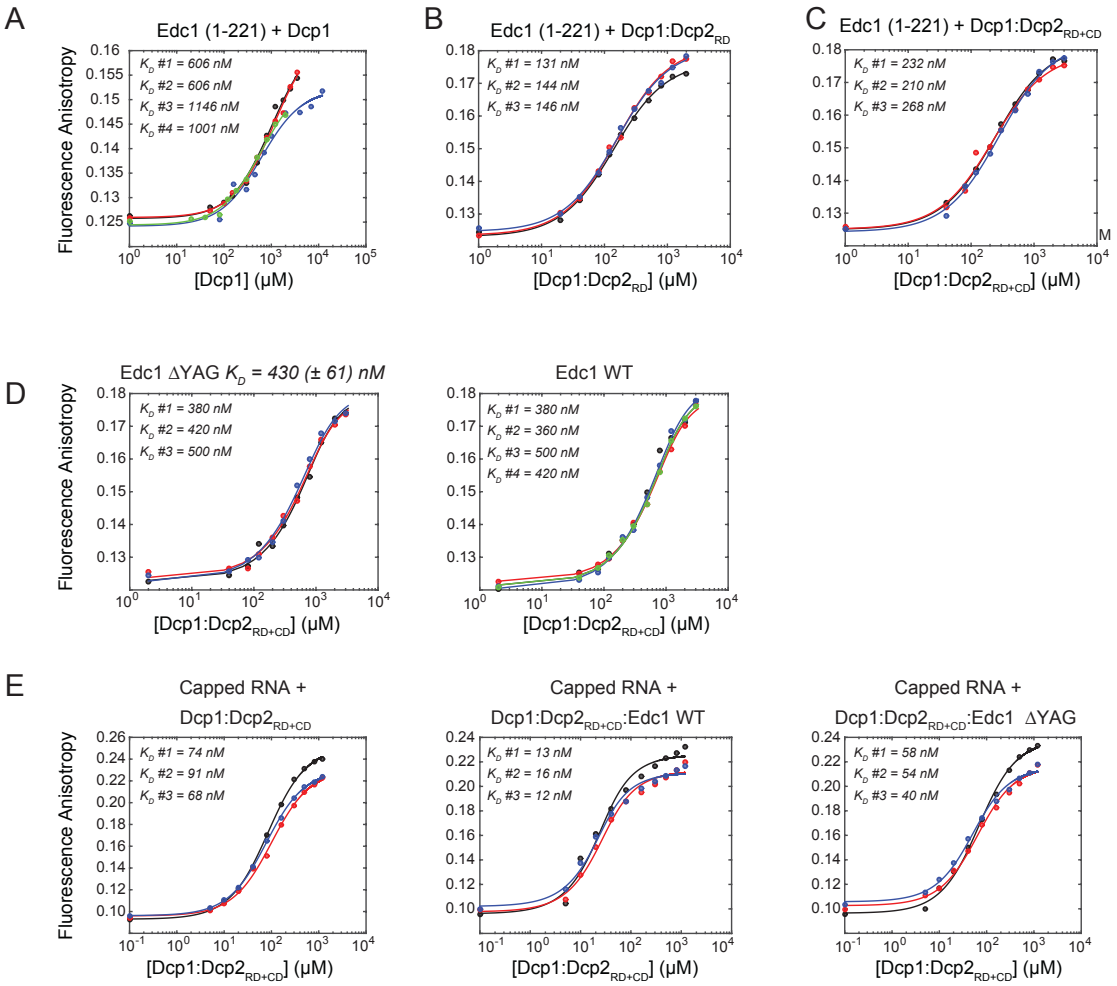

Figure S12. Overview of the recorded binding data (see Figure 4 in the main text for details). The data is represented as a semi-log graph, where the lowest protein concentration (no protein) has been adjusted to 10^0 or 10^{-1} for data presentation purposes.